A Thermodynamic Criterion for Selection of Gas Compositions for Diamond Deposition

K.T. Jacob[1], Namrata Gundiah[1] and A.G. Menon[2]

[1]*Materials Research Center and* [2]*Instrumentation and Services Unit*
Indian Institute of Science, Bangalore - 560 012, India

ABSTRACT

Isoactivity lines for carbon with respect to diamond as the standard state have been calculated in the ternary system C-H-O at 1223 K to identify the diamond deposition domain. The gas composition is calculated by suppressing the formation of all condensed forms of carbon using the SOLGASMIX free-energy minimization program. Thirty six gas species were included in the calculation. From the gas composition, isoactivity lines are computed using recent data on the Gibbs energy of diamond. Except for activities less than 0.1, the isoactivity lines are almost linear on the C-H-O ternary diagram. Gas compositions which generate activity of diamond ranging from 1 to 100 at 1223 K fall inside a narrow wedge originating from the point representing *CO*. This wedge is very similar to the revised lens-shaped diamond growth domain identified by Bachman *et al.*, using inputs from experiment. The small difference between the calculated and observed domains may be attributed to variation in the supersaturation required for diamond deposition with gas composition. The diamond solubility in the gas phase along the isoactivity line for a_{di} = 100 and P = 6.7 kPa exhibits a minimum at 1280 K, which is close to the optimum temperature found experimentally. At higher supersaturations, non-diamond forms of carbon, including amorphous varieties, are expected. The results suggest that thermodynamic calculations can be useful for locating diamond growth domains in more complex CVD systems containing halogens, for which very little experimental data is available.

1. INTRODUCTION

The superior and in many respects unsurpassed physical properties of diamond and the feasibility of growing diamond as a film or a coating using chemical vapor deposition (CVD) techniques are expected to lead to a rapid increase in technological applications of this material. Bachmann *et al.* /1/ have observed that gas compositions in the system C-H-O which have been reported to deposit diamond fall within a well defined region of the ternary phase diagram as shown in Fig. 1. This region is independent of both the type of carbon-containing species admitted to the reactor as well as the growth method. Inputs for the construction of the diagram came from more than eighty deposition experiments reported in over twenty five references. There are no reports of diamond growth in the oxygen-rich region of the diagram. Non-diamond carbon deposition is observed in the carbon-rich region. The empirical observations of Bachmann *et al.* /1/ suggests the existence of some thermodynamic constraints on gas composition for diamond deposition.

The diamond deposition domain has subsequently been redefined by Bachmann *et al.* /2/ in the light of more recent experiments. In many of the earlier studies, the gas compositions were not controlled with sufficient accuracy. The revised diagram is shown in Fig. 2. The narrow deposition region suggests the need for very accurate control of gas composition in these experiments. The frequently reported irreproducibility of data is probably on account of the absence of such fine control.

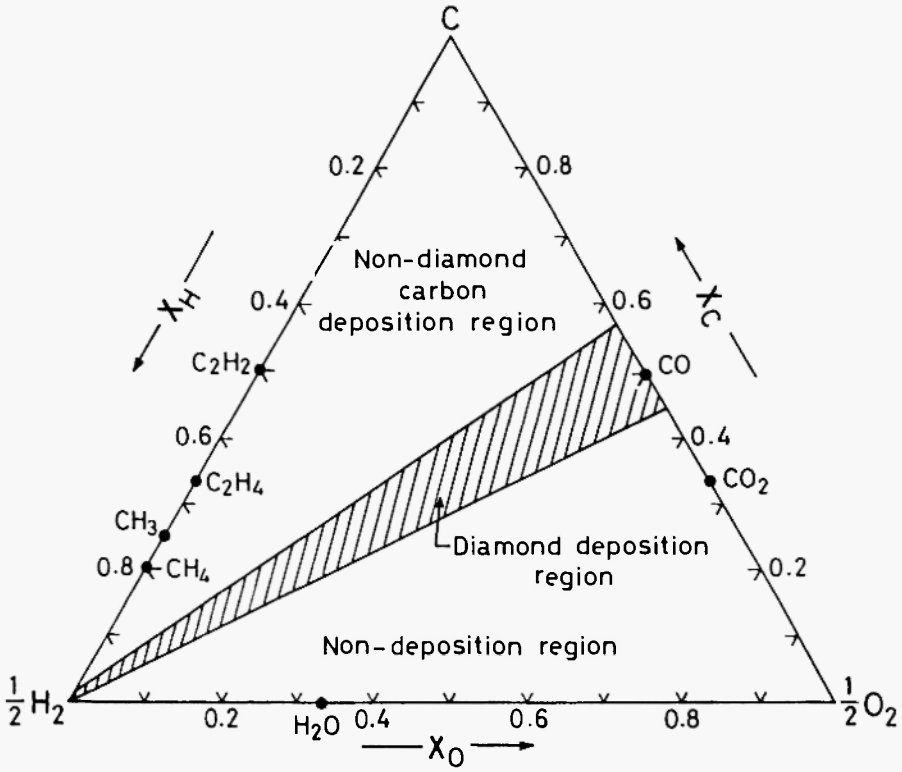

Fig. 1: The Gibbs triangle representation of gas compositions in the ternary system C–H–O which have been found to deposit diamond by low pressure CVD techniques (after Bachmann *et al.* /1/).

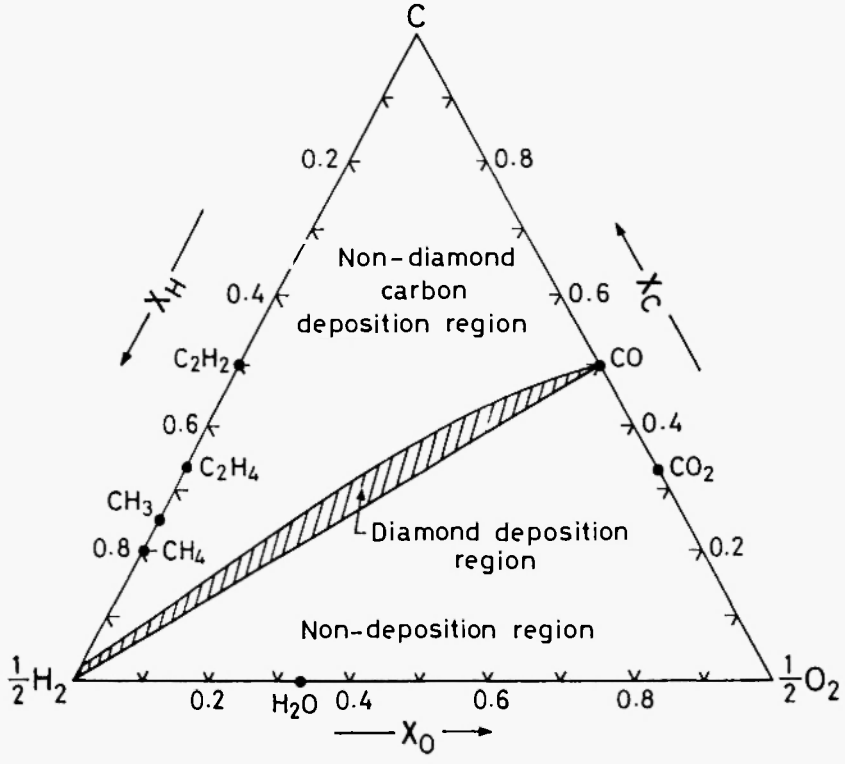

Fig. 2: Refined Bachmann *et al.* /2/ diagram showing a lens-shaped diamond deposition region established by more recent experiments.

The purpose of this paper is to explore the thermodynamic factors responsible for the empirical observations of Bachmann and coworkers /1,2/. An understanding of the basic rules that define the narrow lens-shaped composition domain /2/ on the Gibbs triangle will enable the construction of similar diagrams for other potential chemical systems for diamond CVD, such as C-H-Cl, C-H-F and C-H-O-Cl(F), where experimental data are either scarce or nonexistent.

It is recognized that the correct gas composition does not necessarily result in diamond deposition. Other parameters controlling the process, such as pressure, energy density in the activation zone, substrate temperature and surface preparation of the substrate, have to be optimized. Although global equilibrium does not exist in the CVD reactor, approach to partial equilibrium involving major chemisorbing hydrocarbon species may occur at the gas/solid interface in view of the slow rate of deposition.

2. METHOD

To explore gas compositions that can deposit diamond, equilibrium calculations are performed on an isolated gas phase, suppressing the formation of all forms of solid carbon. Composition of the gas in internal equilibrium at a given temperature and pressure, which can be computed using a free energy minimization routine, will determine if the gas phase is unsaturated, saturated or supersaturated with respect to the various condensed forms of carbon. The activity of solid carbon with respect to either graphite or diamond can be calculated from the equilibrium gas composition and the free energies of graphite and diamond. In the deposition domain, the gas is always supersaturated, with the activity of carbon greater than unity. Thus the deposition domains for graphite and diamond can be independently mapped from equilibrium distribution of species in the gas phase. The deposition region for diamond would be a subset of that for graphite since, at low pressure and moderate temperature, graphite is a stable form of carbon compared to diamond. However, the procedure permits an independent demarcation of the diamond boundary within the graphite domain.

The program SOLGASMIX /3,4/ is used to compute the equilibrium composition of various species in the isolated gas phase. It uses Lagrange's method of undetermined multipliers and the method of steepest descent to find the minimum free energy of a constrained system. The Gibbs free energy of the gas, G, is a function of moles of each specie present. The free energy minimization is carried out subject to mass balance for specific elemental inputs. A set of initial guess values for the composition is assumed. They are subsequently improved in each iteration.

The chemical potential of any form of carbon in the gas phase with reference to a chosen standard state is determined by the partial pressures of various species present in the gas phase at equilibrium. The activity may be calculated from the ratio of the partial pressures of pure carbon species in the gas phase to its equilibrium vapour pressure over the allotropic form of carbon chosen as the standard state. Thus the activity of carbon relative to graphite as the standard state, a_{gr}, is given by

$$a_{gr} = \frac{P_C}{P^o_{C(gr)}} = \left(\frac{P_{C_2}}{P^o_{C_2(gr)}}\right)^{\frac{1}{2}} = \cdots = \left(\frac{P_{C_n}}{P^o_{C_n(gr)}}\right)^{\frac{1}{n}} \quad (1)$$

Similarly, the activity of carbon relative to diamond as the standard state, a_{di}, can be computed at any temperature using the relations:

$$a_{di} = \frac{P_C}{P^o_{C(di)}} = \left(\frac{P_{C_2}}{P^o_{C_2(di)}}\right)^{\frac{1}{2}} = \cdots = \left(\frac{P_{C_n}}{P^o_{C_n(di)}}\right)^{\frac{1}{n}} \quad (2)$$

where $P^o_{C_n(gr)}$ and $P^o_{C_n(di)}$ are the equilibrium vapour pressures of the carbon species C_n over pure graphite and diamond, respectively. Since the partial pressures of carbon species are extremely small, the activity calculated using the above ratios may be distorted by truncation effects. It is advantageous to use partial pressures of major constituents of the gas phase to compute activity of carbon relative to a specific form. For example, the equilibrium:

$$C(di) + 2H_2(g) \rightleftharpoons CH_4(g) \quad (3)$$

can be used to compute the activity of carbon relative to diamond in the gas phase from equilibrium partial pressures of H_2 and CH_4;

$$a_{di} = \frac{exp(\Delta G_3^o/RT)(P_{CH_4})}{P_{H_2}^2} \quad (4)$$

The standard Gibbs free energy change for reaction (3), ΔG_3^o, is obtained by combining the standard free energy of formation of $CH_4(g)$ from graphite and diatomic hydrogen gas, according to the reaction,

$$C(gr) + 2H_2(g) \rightleftharpoons CH_4(g) \quad (5)$$

ΔG_5^o, given in standard tables /5/, with the results of recent determination /6/ of the Gibbs free energy of diamond relative to graphite:

$$C(gr) \rightleftharpoons C(di) \quad (6)$$

$$\Delta G_6^o = \mu_{C(di)}^o - \mu_{C(gr)}^o = \quad (7)$$

$$1100 + 4.64T \quad (\pm 50) \quad Jmol^{-1}$$

Eqn. (3) is obtained by combining eqns. (5) and (6). Therefore,

$$\Delta G_3^o = \Delta G_5^o - \Delta G_6^o \quad (8)$$

The SOLGASMIX program /3,4/ is used to compute the equilibrium partial pressures in the isolated gas phase, wherein the formation of solid carbon is suppressed. This is done by setting the number of condensed phases to zero. The isoactivity lines for diamond spanning the Gibbs triangle for the system C–H–O at constant temperature are computed by appending a subroutine to the SOLGASMIX program. As shown in Fig. 3, along lines connecting points on the base of the Gibbs triangle representing the binary H-O to the vertex representing C, the ratio of mole fraction of hydrogen to oxygen (X_H / X_O) is constant. Along these paths of constant mole fraction ratio, (X_H / X_O), carbon activity increases with the mole fraction of carbon. To locate points on an isoactivity curve for diamond, computations are carried out along lines of constant (X_H / X_o). The equilibrium gas composition is initially calculated for an arbitrary value of X_C using the SOLGASMIX program. Then, activity of carbon relative to diamond is computed by using

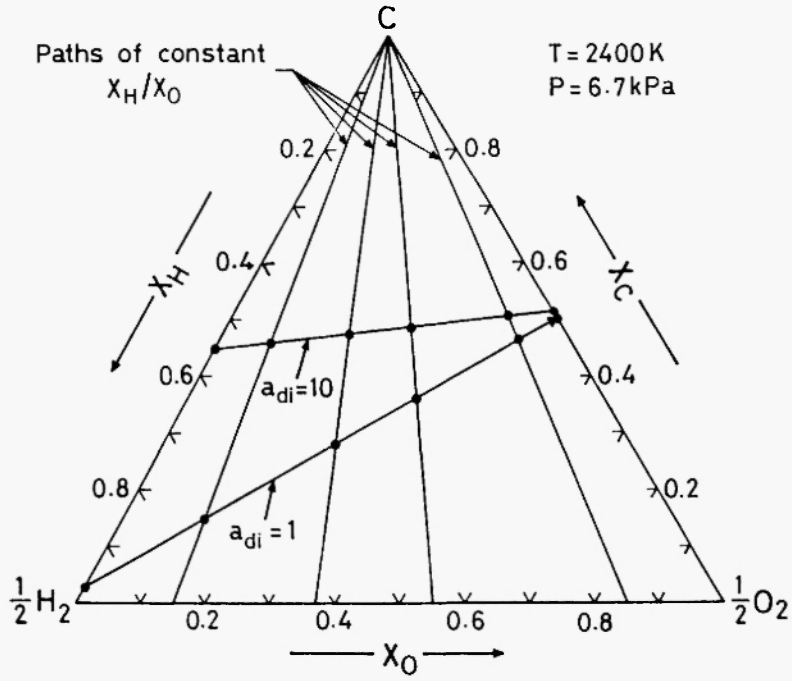

Fig. 3: Paths of constant mole fraction ratio (X_H/X_C) on the ternary triangle. The carbon content of the gas phase is either incremented or decremented along these paths to locate isoactivity lines. Two isoactivity lines at 2400 K and 6.7 kPa pressure are shown.

eqn. (4). If the computed activity is less than that corresponding to the isoactivity curve, X_C is incremented in small steps, keeping (X_H / X_O) constant, till the desired value of activity of carbon is obtained. Similarly, if the initial computation gave a value of activity higher than that for the desired isoactivity curve, X_C is decremented in steps. Computations along several lines originating from the carbon apex, as illustrated in Fig. 3, generates a set of isoactivity curves. The isoactivity lines of Fig. 3 are computed at a temperature of 2400 K and a pressure of 6.7 kPa.

3. DATA INPUTS

SOLGASMIX program /3,4/ requires that the total number of elements, mixtures, pure condensed phases and number of species in each mixture be specified. The additional inputs needed are pressure, system composition and Gibbs energies of all the species included in the computation. In this study, computations are performed for compositions inside the ternary C–H–O system. Thus, only three elements are involved. An ideal gas mixture of 36 species is considered. Table 1 lists the various species and their Gibbs energies of formation at 1223 K. Data from JANAF (1985) tables /5/ are used preferentially. For species not included in the JANAF compilation, data from McBride *et al.* /7/ are used. An error has been detected in the data for $C_2H_2(g)$ in JANAF tables (1985) and the corrected values /8/ are used in the computation. Hydrocarbon species containing more than three carbon atoms have been neglected since they are unlikely to form during the passage of the gas from the activation zone to the substrate in low pressure CVD.

Table 1
Gas Species in the System C–H–O and their Gibbs Free Energies of Formation at 1223 K.

SPECIE	$\Delta_f G^o$ kJ mol^{-1}	SOURCE	SPECIE	$\Delta_f G^o$ kJ mol^{-1}	SOURCE
H_2	0.0	JANAF [5]	$C(V)$	525.268	JANAF [5]
CH	456.670	JANAF [5]	CH_2	320.523	JANAF [5]
CH_3	164.953	JANAF [5]	CH_2OH	76.569	NASA [7]
CH_3O	117.487	NASA [7]	CH_4	44.077	JANAF [5]
CO	-219.818	JANAF [5]	CO_2	-396.116	JANAF [5]
C_2	600.464	JANAF [5]	C_2H	317.788	JANAF [5]
C_2H_2	157.669	REF [8]	C_2H_4	137.366	JANAF [5]
C_2H_4O	131.208	JANAF [5]	C_2H_6	162.380	JANAF [5]
C_2O	137.477	JANAF [5]	C_3	554.353	JANAF [5]
C_4	715.777	JANAF [5]	O_2	0.0	JANAF [5]
H_2O	-180.125	JANAF [5]	H_2O_2	-3.581	JANAF [5]
H	152.695	JANAF [5]	OH	20.126	JANAF [5]
HO_2	57.569	JANAF [5]	H_2CO	-79.701	JANAF [5]
HCO	-14.475	JANAF [5]	C_3O_2	-164.044	JANAF [5]
O	173.107	JANAF [5]	CH_3OH	-19.737	NASA [7]
C_2H_5OH	69.633	NASA [7]	C_3H_6O	216.564	NASA [7]
C_3H_8O	173.806	NASA [7]	C_3H_8O	169.061	NASA [7]
CH_2CO	-37.614	NASA [7]	C_2H_3	279.589	NASA [7]

4. RESULTS AND DISCUSSION

4.1. Isoactivity Contours and Diamond Deposition Domain

The computed isoactivity curves for diamond in the ternary system C–H–O at 1223 K and a total pressure of 6.7 kPa are displayed in Fig. 4. To permit clear identification of the lines in the diagram, only a few selected isoactivity curves are presented. Along each curve the chemical potential of diamond is constant, since $\Delta\mu_{C(di)} = RT\ln a_{di}$. The temperature and pressure chosen are typical conditions at the substrate for diamond deposition. Isoactivity lines for $a_{di} \geq 0.1$ are almost linear. For $a_{di} \geq 1$, the isoactivity lines originate from the composition representing the compound *CO* on the C–O binary and link with a composition on the C–H binary. Therefore, for interpolation between isoactivity lines for $a_{di} \geq 1$, it is sufficient to locate a point on the C–H binary for the desired activity and then connect this point to the *CO* composition by a straight line.

Isoactivity lines in Fig. 4 refer to an isolated gas phase in which the condensation of the solid carbon is prevented. The sum of partial pressures of all carbon species, ΣP_{C_-}, at 1223 K is substantially below the total pressure (6.7 kPa). Because of the large negative value for the standard free energy of formation of CO from C and O_2, the gas phase for $a_{di} \geq 1$ at 1223 K along the C–O binary contains essentially *CO*. Therefore, isoactivity lines shown in the figure for $a_{di} \geq 1$ do not pass through the apex of the Gibbs triangle representing pure carbon.

The activity of carbon in pure diamond, a_{di}, relative to graphite as the standard state at 1223 K, calculated from Eqn. (7), is 1.95. Thus, the isoactivity curves for diamond are also the isoactivity curves for graphite. To obtain the activity of carbon with respect to graphite corresponding to any curve, the value of a_{di} has to be multiplied by 1.95.

The driving force for diamond deposition from the gas phase is the difference in the chemical potential (or activity) of carbon between the gas and diamond. The deposition of diamond can occur only when $a_{di} \geq 1$.

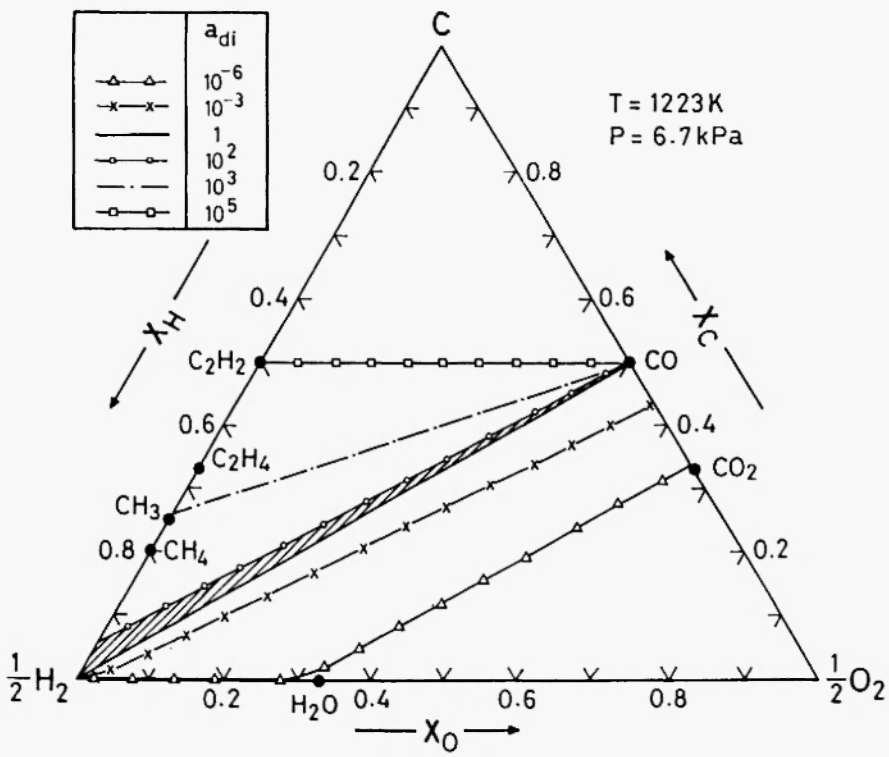

Fig. 4: Isoactivity lines for carbon in the gas phase with reference to diamond as the standard state at 1223 K and 6.7 kPa pressure.

Thus, the no-growth region for diamond at 1223 K is clearly demarcated as the area that lies below the line joining the hydrogen apex to the *CO* composition in Fig. 4. The supersaturation required for the nucleation of diamond is estimated to vary from 10 to 100 depending on the substrate, temperature, pressure, gas composition and specific reaction pathways involved. For gas compositions close to the C–H binary, the supersaturation needed for diamond deposition is 10, while for compositions richer in oxygen higher supersaturation is needed. Carbon has a very high affinity for oxygen compared to hydrogen and all oxygen is essentially tied up with carbon as CO at 1223 K in the diamond deposition region. Since diamond deposition occurs from hydrocarbon precursors, the presence of stable *CO* species increases the supersaturation required for diamond deposition. The range of gas compositions corresponding to $1 \leq a_{di} < 100$ can be accommodated inside the hatched wedge-shaped region in Fig. 4. This region is very similar to that suggested by Bachmann and coworkers /2/ based on experimental information from the literature spanning a quarter of a century of worldwide diamond CVD research. The experimental domain for diamond is shown in Fig. 2.

The Bachmann domain /2/ for diamond deposition is somewhat wider in the middle and narrower near the C–H boundary as compared to the computed wedge. The small difference is at least partly related to the variation of supersaturation required for deposition with composition of the gas. At supersaturations significantly greater than 100, non-diamond carbons including amorphous varieties are expected. Thus, the experimental observations from a variety of sources are in accord with the partial equilibrium calculations at the substrate temperature, suppressing the formation of graphite. The close correspondence between the calculated and empirically determined domains is found regardless of the deposition technique used and the chemical composition of the source gases. The striking feature is not the small discrepancy between the calculated domain for diamond deposition and that suggested by Bachmann *et al.* /2/ based on compiled experimental data, but the broad agreement between the two. In view of the non-equilibrium nature of the CVD process, the broad agreement between calculations based on partial equilibrium between diamond and the gas phase and experimental data is indeed surprising. The supersaturation referred to in this paper is of chemical origin, resulting from readjustment of equilibria involving the various species in the gas phase. Supersaturation resulting from supercooling of the gas phase, such as that present during physical vapour deposition, is not considered. The gas phase reactions are assumed to proceed sufficiently rapidly to permit the gas to be in internal equilibrium.

The wider the deposition domain, the easier it is to control the deposition process. Small fluctuations in the gas composition during experiment can be tolerated better when the width of the domain is larger. Since the deposition region narrows to a point on the binary C–O at 1223 K, the thermodynamic analysis indicates that it is practically impossible to grow diamond from gas compositions lying exclusively on this binary. There have been no reports of successful diamond growth using a mixture of *CO* and CO_2.

Since graphite is more stable than diamond, it is also expected to codeposit with diamond. The rates of deposition of diamond and graphite would be governed by mechanistic and kinetic factors which are not discussed in this paper. Presence of atomic hydrogen in the gas phase appears to be necessary to etch away the graphite preferentially and produce a good diamond film. Chemisorbed hydrogen on the diamond surface partially protects diamond from etching by atomic hydrogen.

4.2 Effect of Temperature on the Deposition Domain

The effect of temperature on the deposition wedge ($1 < a_{di} < 100$) at a pressure of 6.7 kPa is shown in Fig. 5. The wedge is wider at 1100 K than at 1300 K. At 800 K, the wedge transforms to a quadrilateral. A range of $CO + CO_2$ mixtures can generate activity of diamond between 1 and 100 at 800 K. Thus, from a thermodynamic point of view, growth of diamond from $CO + CO_2$ mixtures becomes feasible at lower temperatures.

Since isoactivity curves in the range 1 to 100 are essentially linear, it is instructive to focus on the variation of isoactivity lines with temperature along the two binaries. The mole fraction of carbon in the gas

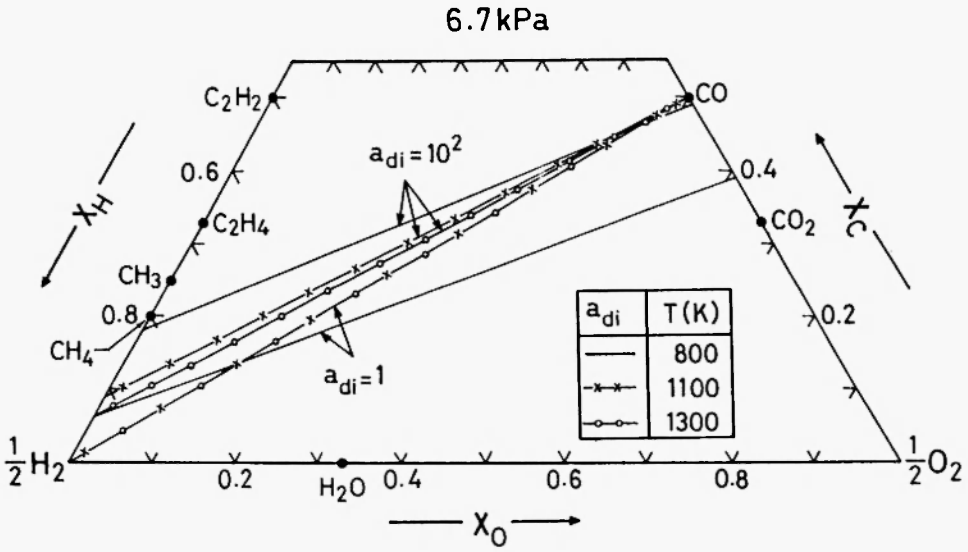

Fig. 5: Effect of temperature on the computed diamond deposition domain at a pressure of 6.7 kPa. The domain is bounded by isoactivity lines correponding to $a_{di} = 1$ and $a_{di} = 100$.

phase for various supersaturations is plotted in Fig. 6 as a function of temperature in the binary system C–H at a pressure of 6.7 kPa. The carbon is distributed between various species present in the gas. The isoactivity curve for $a_{di} = 100$ shows a minimum in carbon solubility of the gas phase at a temperature of 1280 K. This solubility minimum signals the optimum temperature for diamond deposition at a pressure of 6.7 kPa. The temperature is sufficiently high to allow the deposition reactions to proceed at reasonable rates. The temperature corresponding to the minimum in carbon solubility is dependent on the total pressure.

The minimum in carbon solubility at $a_{di} = 100$ is caused by decreasing the concentration of CH_4 and increasing the concentration of C_2H_2 with increasing temperature. This is clearly illustrated in Fig. 7, where

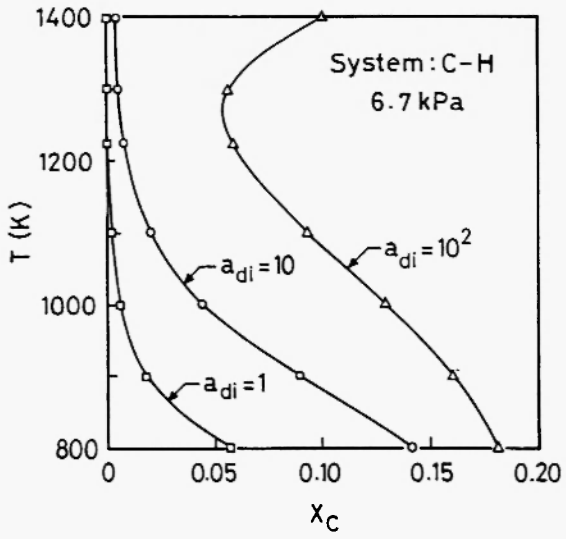

Fig. 6: Variation of the mole fraction of carbon in the gas phase with temperature for various activities of diamond in the binary system C–H at pressure of 6.7 kPa.

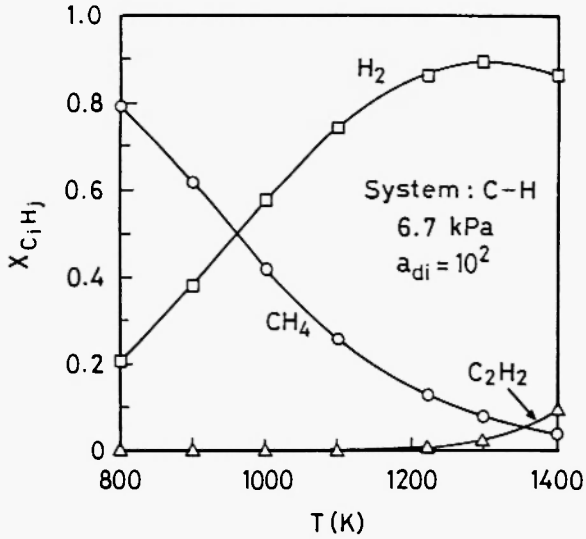

Fig. 7: Variation of the mole fraction of the major hydrocarbon species (C_iH_j) with temperature in the binary system C–H at a pressure of 6.7 kPa and $a_{di} = 100$.

the concentration of major carbon-containing species is plotted as a function of temperature. On the ternary triangle, the effect of increasing temperature is to shift the isoactivity line for a_{di} = 100 to lower carbon concentration up to approximately 1280 K. Further increase in temperature causes a reversal and the isoactivity lines move in a direction of increasing carbon content. Although the mole fraction of carbon in the gas phase decreases with increasing temperature for a_{di} = 1 and 10, for the range of temperatures displayed in Fig. 6, minima in the solubility of carbon are obtained at higher temperatures. This can be inferred from combined inspection of Figs. 3 and 6.

4.3. Effect of Pressure on the Deposition Domain

Effect of pressure on the diamond deposition wedge is shown in Fig. 8. The wedge becomes wider with increasing pressure. Although increase in pressure facilitates better control of gas composition, high pressure operations will result in the loss of atomic hydrogen through interatomic or intermolecular collisions in the gas. Atomic hydrogen, produced by activation of the gas phase, is required for etching graphite that invariably codeposits with diamond in the CVD reactor. Hence, an optimum value of pressure has to be established balancing these factors. The isoactivity lines for a_{di} = 1 and 100 shift towards higher carbon concentration with increasing pressure, the shift being more pronounced for a_{di} = 100.

Again, it is instructive to see the effect of pressure on carbon solubility in the gas phase at fixed activity of diamond in the binary C–H system. Fig. 9 indicates a shift to higher carbon content with increasing pressure for a_{di} = 100, and the reversal of this trend for a_{di} = 10^3. As expected from theoretical considerations, the isoactivity lines do not cross. On the Gibbs triangle, the isoactivity lines for a_{di} = 10^3 move in a direction of decreasing carbon content with increasing pressure. To investigate the reason for this reversal, the concentrations of major gas species at the two activities are plotted in Figs. 10 and 11 as a function of pressure. In the binary system C–H at 1223 K, a_{di} = 100 and pressure varying from 1 to 100 kPa, the major species of interest are CH_4 and H_2. Although H_2 is predominant at low pressures, the concentration of CH_4 becomes more significant at higher pressures (Fig. 10). Consequently, the mole fraction of carbon in the gas phase increases with pressure as shown in Fig. 9. At a_{di} = 10^3 and T = 1223K, the major species are CH_4,C_2H_2,C_2H_4 and H_2. At very low pressures, $H2$ and C_2H_2 species predominate (Fig. 11). As the pressure is increased, CH_4 dominates the gas phase. The concentrations of CH_4 and C_2H_4 increase with pressure, while those of H_2 and C_2H_2 decrease. The net effect is a decrease in the mole fraction of carbon in the gas phase with pressure for a_{di} = 10^3.

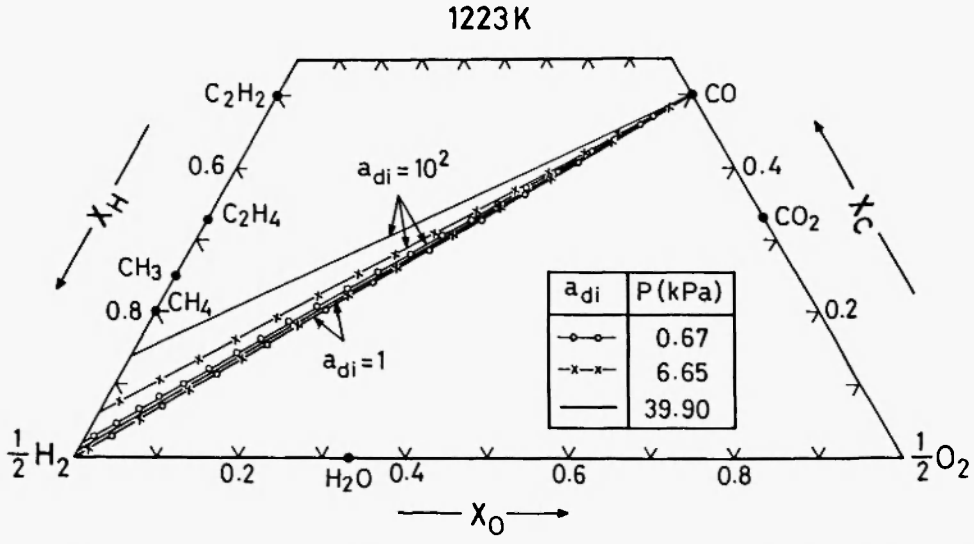

Fig. 8: Effect of pressure on the carbon deposition wedge in the ternary system C–H–O at 1223 K.

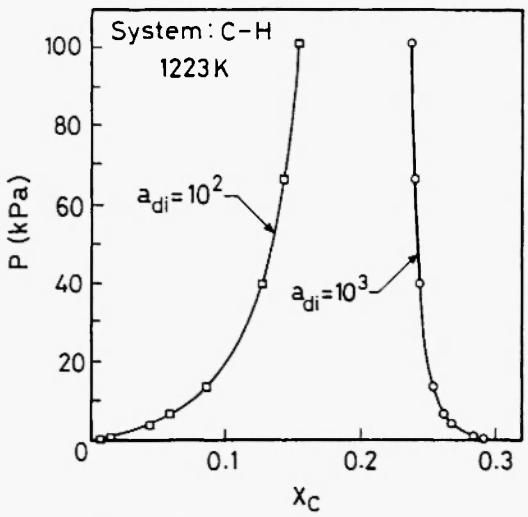

Fig. 9: Effect of pressure on the mole fraction of carbon in the gas phase in the binary system C–H at 1223 K along isoactivity curves corresponding to $a_{di} = 10^2$ and $a_{di} = 10^3$.

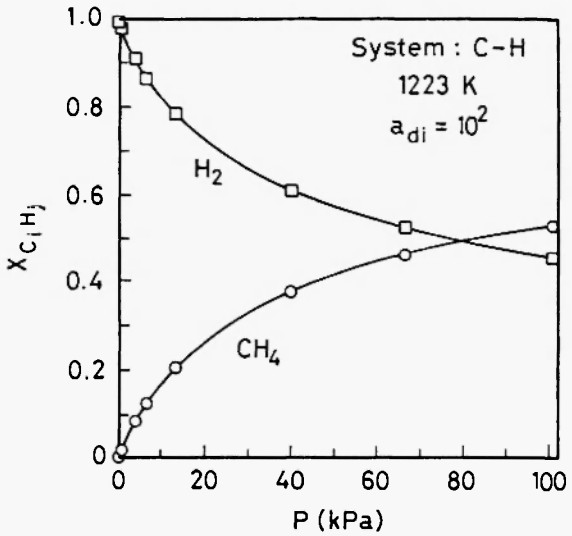

Fig. 10: Variation of the mole fraction of the species CH_4 and H_2 with pressure at 1223 K and a_{di} = 100.

4.4. Comparison with Earlier Computations

Recently, a few attempts have been made to compute the diamond deposition domain using thermochemical data /9,10/. All these calculations are based on graphite as the standard state for carbon. The

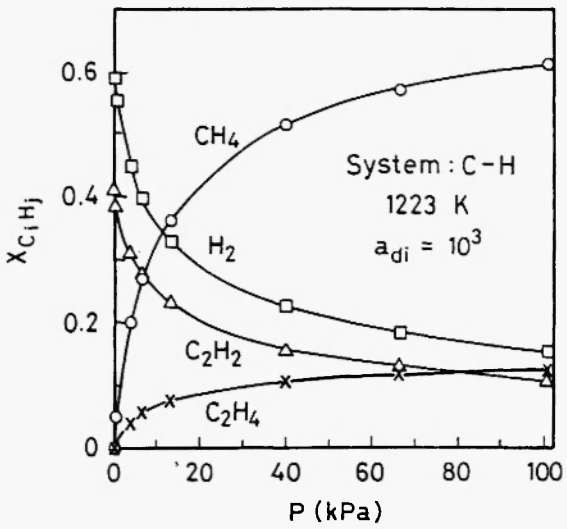

Fig. 11: Effect of pressure on the mole fraction of the species CH_4, H_2, C_2H_2 and C_2H_4 in the binary system C–H at 1223 K and $a_{di} = 10^3$.

chemical potential difference between graphite and diamond /6/ is ignored in these calculations. Hwang *et al.* /9/ showed that the partial pressure of carbon increases with increasing temperature at constant gas composition. They identified a very narrow composition band along the H_2–CO line, where a reasonable amount of supersaturation exists for carbon deposition. On the carbon-excess side of this band, very large supersaturation was encountered, and on the oxygen-excess side the gas was found to be undersaturated with respect to graphite. The deposition domain identified by Hwang *et al.* /9/ is considerably narrower than the lens-shaped region established by experiment /2/ and the wedge-shaped region identified in this study. Since Hwang *et al.* /9/ did not map iso-supersaturation contours across the ternary, they were unable to detect some of the trend reversals with temperature and supersaturation observed in this study. Nevertheless, they showed the importance of thermochemical factors in controlling the deposition.

Prijaya *et al.* /10/ calculated gas compositions in the ternary in equilibrium with graphite as a function of temperature in the range 900-3000 K at a fixed pressure of 5.3 kPa. They found that the carbon content of the gas phase in equilibrium with graphite increases with increasing temperature. Results obtained in this

study indicate that their conclusion is not strictly correct. The carbon solubility exhibits a minimum at a temperature defined by the total pressure and activity of carbon. Since the carbon solubility in the gas phase for activity of graphite, a_{gr} = 1, and P = 5.3 kPa, is very small in the range 1100-2400 K, the minimum may not be apparent unless explored carefully. The successful diamond growing compositions identified by Prijaya *et al.* /10/ are those which are slightly undersaturated with graphite at gas excitation temperatures. As the gas cools on its approach to the substrate, modest super-saturations are achieved as a result of a shift in equilibrium, thus providing the necessary condition for diamond growth. Mostly the gas phase computations of Prijaya *et al.* /10/ pertain to the gas excitation temperature, rather than the temperature of the substrate where deposition occurs. They have computed contours of constant species concentration at 2500 K in an attempt to identify the important species involved in the deposition process.

4.5. Comparison with Experiment

Several techniques have been used to measure the gas composition in the CVD process for diamond. The various methods can be broadly grouped into three categories: sample extraction techniques, physical probes and optical probes. In the first category, a sample of the gas extracted from the CVD reactor is analysed by gas chromatography (GC), mass spectro-metry (MS) and matrix-isolation Fourier transform infrared spectroscopy (MI-FTIR), Langmuir probe (LP) and thermocouple (TC) are examples of physical probes deployed in experimental reactors. Optical emission spectroscopy (OES), laser-induced fluorescence (LIF), resonance-enhanced-multiphoton ionization (REMPI), Fourier transform infrared spectroscopy (FTIR), infrared diode laser absorption spectroscopy (IR-DLAS), coherent anit-Stokes Raman spectroscopy (CARS) and third harmonic generation (THG) are among the optical probes used for gas phase diagnosis. None of these techniques are applicable for the detection of all species in every CVD environment. Often, compromises have to be made between the species being monitored, the information required, the reactive environment probed and the diagnostic technique.

Since thermodynamic computation suggests approach to partial equilibrium near the substrate, it would be useful to compare computed gas compositions with that existing in the reactor in the close vicinity of the substrate. Unfortunately, none of these techniques are suitable for obtaining accurate site-specific gas composition in the reactor. Hsu *et al.* /11/ have used molecular beam mass spectrometry (MBMS) to detect concentration of the species near the substrate. The gas is extracted through a knife-edge orifice on the substrate by applying a differential pressure across the substrate. The mass spectrometric analysis would be a representative of the gas phase approaching the substrate from the activation zone, but not necessarily in partial or local equilibrium with the substrate. The computed concentration of major species at 1100 K and a pressure of 2.66 kPa is compared with the measurements of Hsu *et al.* in Table 2 for input H_2 gas containing 7.4% CH_4 and 6.7% Ar. There is agreement between calculated and measured concentrations of CH_4, H_2 and Ar. There is an order of magnitude difference for the C_2H_2 species. The computed concentrations of CH_3 and H are several orders of magnitude lower than the values determined by mass spectrometry. The H_2 and Ar species show almost the same value. Since chemical potentials of CH_3 and C_2H_2 species in the gas approaching the substrate from the activation zone are significantly higher than the equilibrium values, it is quite likely that they participate in reactions leading to diamond deposition. Both methyl and acetylene addition mechanisms have been proposed by several investigations and a recent summary is given by Spear and Frenklach /12/. A combined CH_3–C_2H_2 mechanism for interdependent addition of both species has also been discussed by these authors.

The rate of deposition of diamond in the CVD process is of the order of 2 μm/hr. This implies that the residence time of the adsorbed hydrocarbon species on the surface is relatively long, allowing approach to local equilibrium. Improved techniques for analysing the composition of the gas phase immediately above the substrate are required to verify this hypothesis.

Table 2
Comparison of Measured and Computed Concentrations of Major Species at 1100 K and 2.66 kPa Pressure for the System C-H-Ar

COMPOSITION OF GAS PHASE	MAJOR SPECIES	COMPOSITION /MOLE FRACTION	
		MEASURED HSU et al [11]	COMPUTED
	H_2	0.90	0.86
7.4 % CH_4	Ar	0.07	0.067
+	CH_4	6.0×10^{-2}	7.3×10^{-2}
6.7 % Ar	CH_3	1.3×10^{-3}	2.7×10^{-7}
+	C_2H_2	6.4×10^{-3}	1.4×10^{-4}
85.9 % H_2	H	1.2×10^{-4}	1.5×10^{-7}

4.6. Gas Composition and Quality of Diamond Film

The rate of diamond deposition is expected to increase with the driving force governing the process if the mechanism remains unaltered. Hence, the higher the activity or chemical potential of diamond in the gas phase, the faster would be the rate of deposition. However, the quality of diamond improves as the rate of deposition decreases. Thus, an optimum composition in the diamond deposition domain can be chosen depending on the application and product specification.

A wear-resistant coating of diamond can be grown using gas mixtures belonging to either C–H or C–H–O systems. It has been observed that the rate of deposition is faster and the crystal quality better when C–H–O mixtures are used. However, connectivity between grains and thermal conductivity are better in films grown from C–H mixtures. Small pores are often present between grains in films grown from C–H–O mixtures. Important properties of the film for wear-resistant applications can be controlled by adjusting the supersaturation in the gas phase. Well-faceted, high-friction diamond is deposited at lower supersaturation. Thus the proper position of the gas composition across the width of the diamond domain is one of the important factors in obtaining diamond films of desired quality. It would also be interesting to study the effect of cycling the activity of diamond in the gas phase between 1 and 100 on the quality of diamond produced.

5. CONCLUSION

The diamond deposition domain for the system C–H–O at 1223 K is computed assuming internal equilibrium in the gas phase. The domain is bounded by two isoactivity curves for diamond, one for $a_{di} = 1$ and the other for $a_{di} = 100$. Recent data /6/ on the chemical potential of carbon in diamond relative to graphite are used in this computation. All prior thermodynamic computations /9,10/ were based on graphite as the standard state for carbon. The computed domain is in broad agreement with the Bachmann domain /2/, which is based on a thorough analysis of experiments using thermal CVD, hot filament CVD, various plasma techniques and combustion flames reported in the literature during the past quarter century. The effects of pressure and substrate temperature on the gas composition domain for diamond deposition are delineated. Subtle changes in gas chemistry and some trend reversals as a function of temperature and supersaturation, undetected in earlier computations /9,10/, are observed while traversing the ternary along isochemical-potential tracks.

Chemical thermodynamics appears to be useful in identifying the window for diamond deposition on the composition diagram for the gas phase. Despite the complex chemistry of the CVD processes and the presence of significant thermal gradients, diamond deposition is restricted to gas compositions that have

the necessary supersaturation at the substrate temperature. Thermodynamic factors seem to be primarily responsible for defining the gas composition domain conducive to deposition. No specific starting materials are required for diamond deposition. Process patents for CVD diamond based on specific starting compounds and mixing ratios fall into oblivion in the light of the general thermodynamic principles governing the process.

The analysis presented in this study not only provides a specific basis for rationalizing experimental information on the C–H–O system, but also suggests a strategy for diamond search in other chemical systems, especially those containing halogens. Optimization of certain properties of the diamond film can also be achieved by choosing the correct composition in the deposition domain. It must be remembered, however, that correct gas composition is a necessary but not a sufficient condition for diamond deposition.

REFERENCES

1. P.K. Bachmann, D. Leers and H. Lydtin, *Diamond Relat. Mater.*, **1**, 1 (1991).
2. P.K. Bachmann, H.J. Hagemann, H. Lade, D. Leers, F. Picht, D.U. Wiechert and H. Wilson, *Mat. Res. Soc. Symp. Proc.*, **339**, Materials Research Society, Pittsburgh, PA, U.S.A., 194; pp. 267.
3. G. Eriksson, *Chimica Scripta*, **8**, 100 (1975).
4. T.M. Bessmann, *"SOLGASMIX – PV", a computer program to calculate equilibrium relationships in complex systems*, ORNL/TN 5775, Oak Ridge National Lab., Tenn., U.S.A., 1977.
5. M.W. Chase, Jr., C.A. Davies, J.R. Downey, Jr., D.J. Frurip, R.A. McDonald and A.N. Syverud, JANAF Thermochemical Tables, 3rd Ed., *J. Phys. Chem. Ref. Data*, **14**, Suppl. 1, Parts I and II (1985).
6. K.T. Jacob, *Solid State Comm.*, **94**, 763 (1995).
7. B.J. McBride, S. Gordon and M.A. Reno, *NASA Technical Memorandum 4513*, NASA Scientific and Technical Information Program, Hampton, U.S.A., 1993.
8. N. Gundiah, K.T. Jacob and A.G. Menon, *Calphad*, **20** (1996) [in press].
9. N.M. Hwang, J.H. Hahn and G.W. Bahng, *Diamond Relat. Mater.*, **3**, 167 (1993).
10. N.A. Prijaya, J.C. Angus and P.K. Bachmann, *Diamond Relat. Mater.*, **3**, 129 (1993).
11. W.L. Hsu, M.C. McMaster, M.G. Coltrin and D.S. Dandy, *Jpn. J. Appl. Phys.*, **33**, 2231 (1994).
12. K.E. Spear and M. Frenklach, *Pure Appl. Chem.*, **66**, 1773 (1994).